

MIT Open Access Articles

*Synthesis of j-aggregating
dibenz[a,j]anthracene-based macrocycles*

The MIT Faculty has made this article openly available. **Please share** how this access benefits you. Your story matters.

Citation: Chan, Julian M. W. et al. "Synthesis of j-aggregating dibenz[a,j]anthracene-based macrocycles." *Journal of the American Chemical Society* 131.15 (2009): 5659–5666.

As Published: <http://dx.doi.org/10.1021/ja900382r>

Publisher: American Chemical Society (ACS)

Persistent URL: <http://hdl.handle.net/1721.1/74239>

Version: Author's final manuscript: final author's manuscript post peer review, without publisher's formatting or copy editing

Terms of Use: Article is made available in accordance with the publisher's policy and may be subject to US copyright law. Please refer to the publisher's site for terms of use.



**Synthesis of J-Aggregating Dibenz[a,j]anthracene-Based
Macrocycles**

Journal:	<i>Journal of the American Chemical Society</i>
Manuscript ID:	ja-2009-00382r.R1
Manuscript Type:	Article
Date Submitted by the Author:	
Complete List of Authors:	Chan, Julian; Massachusetts Institute of Technology Tischler, Jonathan; MIT, Electrical Engineering and Computer Science Kooi, Steven; MIT, ISN Bulovic, V.; MIT, Electrical Engineering and Computer Science Swager, Timothy; Mass. Inst. of Tech., Chemistry



Synthesis of J-Aggregating Dibenz[*a,j*]anthracene-Based Macrocycles

*Julian M. W. Chan, Jonathan R. Tischler, Steve E. Kooi, Vladimir Bulović, Timothy M. Swager**

Department of Chemistry and Department of Electrical Engineering and Computer Science,

Massachusetts Institute of Technology, 77 Massachusetts Avenue, Cambridge, Massachusetts 02139

e-mail: tswager@mit.edu

RECEIVED DATE (to be automatically inserted after your manuscript is accepted if required according to the journal that you are submitting your paper to)

ABSTRACT. Several fluorescent macrocycles based on 1,3-butadiyne-bridged dibenz[*a,j*]anthracene sub-units have been synthesized via a multistep route. The synthetic strategy involved the initial construction of a functionalized dibenz[*a,j*]anthracene building block, subsequent installation of free alkyne groups on one side of the polycyclic aromatic framework, and a final cyclization based on a modified Glaser coupling under high-dilution conditions. Photophysical studies on three conjugated macrocycles revealed the formation of J-aggregates in thin films as well as in concentrated solid solutions (polyisobutylene matrix) with peak absorption and emission wavelength in the range of $\lambda = 460$ nm to $\lambda = 480$ nm. The characteristic red-shifting of the J-aggregate features as compared to the monomer spectra, enhancement in absorption intensities, narrowed linewidths, and minimal Stokes shift values, were all observed. We demonstrate that improvements in spectral features can be brought about by annealing the films under a solvent-saturated atmosphere, where for the best films the luminescence quantum efficiency as high as 92% was measured. This class of macrocycles represents a new category

1 of J-aggregates that due to their high peak oscillator strength and high luminescence efficiency have the
2 potential to be utilized in a variety of optoelectronic devices.
3
4
5

6 INTRODUCTION. Shape-persistent macrocycles have received much attention in the field of materials
7 science, particularly in the area of nanoscale architectures.¹ The first macrocycle featuring two
8 unfunctionalized anthracenes linked by 1,3-butadiyne bridges was reported in 1960, but due to the lack
9 of modern synthetic and characterization methods, the nature of the resulting material was not rigorously
10 elucidated.² Following little interest in such systems over the next four decades, reports of anthrylene-
11 ethynylene oligomers and macrocycles have surfaced in the past 5 years.³ However, the molecular
12 rigidity and lack of solubilizing groups resulted in the reported compounds having poor solubilities in
13 common solvents. To create a class of molecules that could have potentially interesting photophysical
14 and materials properties, we embarked on the design of conjugated macrocycles based on rigid
15 dibenz[*a,j*]anthracene units bridged by butadiyne π -linkers. This was a logical choice since
16 aryleneethynylene and 1,3-butadiyne linkages are frequently used in conjugated systems (e.g. polymers)
17 for their ability to maintain rigidity and π -conjugation.⁴ The polycyclic aromatic motifs are commonly
18 seen in other areas of materials science, notably in the fields of discotic liquid crystals and graphitic
19 materials.⁵ By employing various modern synthetic transformations, it was possible to introduce
20 numerous functionalities (e.g. sidechains) into the structure to give better solubility and processability.
21 In particular, bulky 4-alkoxyphenyl substituents located near the middle of the macrocycles serve several
22 purposes: 1) as synthetic handles to allow for the facile electrophilic cyclizations⁶ used to establish the
23 dibenz[*a,j*]anthracene framework, 2) as solubilizing groups, and most importantly, 3) as a source of
24 steric hindrance to bring about twisting of the π -system. Such distortion of the rigid framework by steric
25 bulk has been known to induce slipped stacking arrangements,⁷ resulting in aggregate structures with
26 unique optical properties. Similar slipped structures are also known in nature: for example, the
27 arrangement of J-aggregated chlorophyll chromophores is crucial to the light-harvesting efficiency of
28 photosynthetic systems.⁸ Using natural photosystems as a guide and inspiration, researchers have found
29
30
31
32
33
34
35
36
37
38
39
40
41
42
43
44
45
46
47
48
49
50
51
52
53
54
55
56
57
58
59
60

ways to emulate this J-aggregate design in various porphyrins and perylene bisimides.⁹ More recently, the laboratories of Frank Würthner have also successfully implemented the rational synthesis of several J-aggregated systems using supramolecular design principles.¹⁰ Ever since their serendipitous discovery in 1936, J-aggregates have been of great theoretical interest because they display coherent, cooperative phenomena like superradiance and giant oscillator strength, a consequence of their electronic excitation being delocalized over several molecules.¹¹ Besides being theoretical curiosities, J-aggregates also have a myriad of practical applications, such as their use as organic photoconductors,¹² photopolymerization initiators,¹³ and nonlinear optical devices,¹⁴ as well as the emerging applications such as the recently demonstrated critically coupled resonators¹⁵ and strongly QED coupled microcavity LEDs.¹⁶

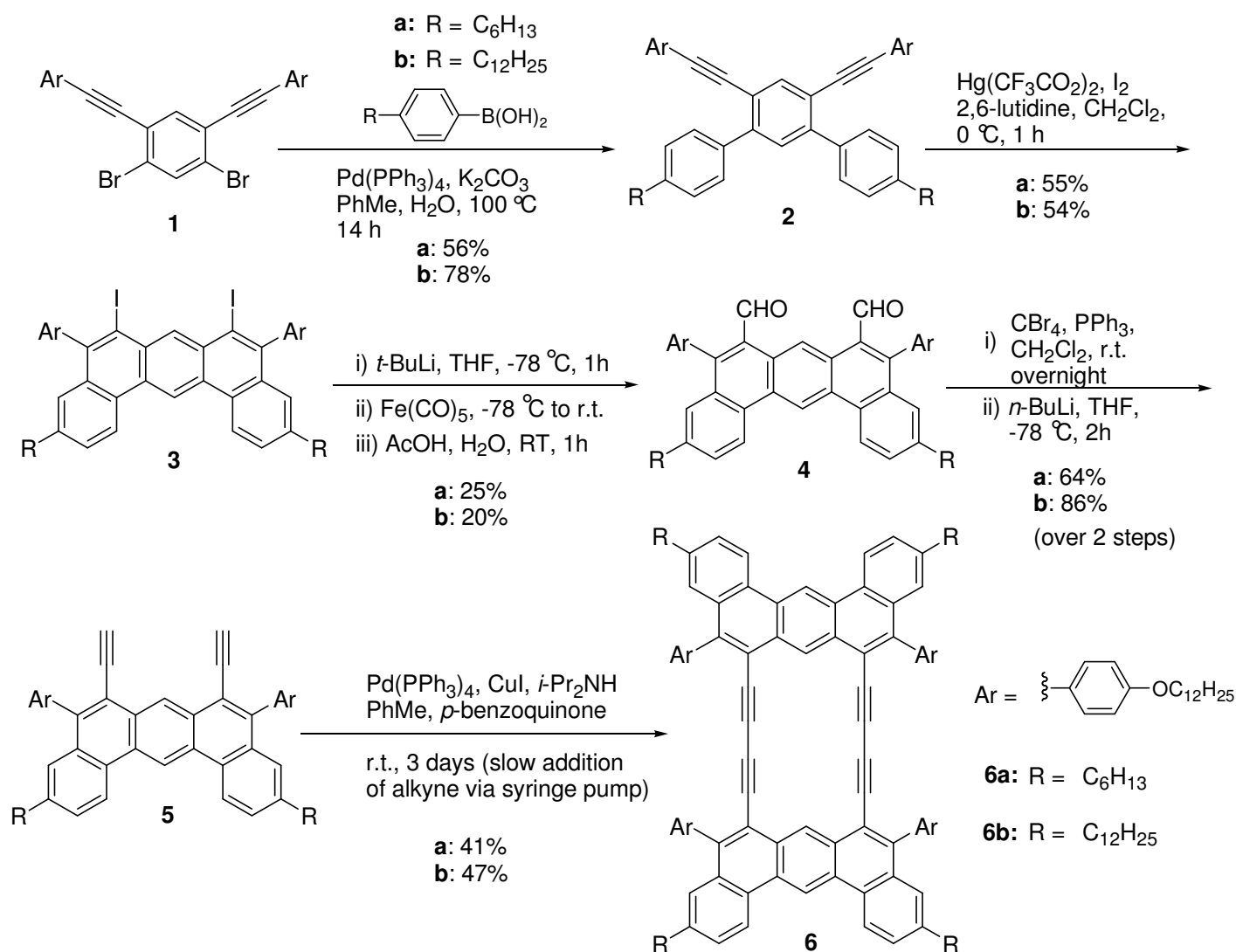
Herein, we report the synthesis and characterization of a series of J-aggregating macrocycles based on functionalized dibenz[*a,j*]anthracene fragments linked at the 6- and 8- positions by a pair of 1,3-butadiyne bridges, in which the ring interior can be viewed as an octadehydro[18]annulene system. The results of their photophysical studies are also detailed.

RESULTS AND DISCUSSION.

Synthesis. Macrocycles **6a** and **6b** were prepared in six steps from the previously reported dibromide **1**¹⁴ (Scheme 1). Subjecting the dibromide to a double Suzuki coupling with 4-alkylphenylboronic acids afforded terphenyl derivatives **2**, which were then converted to the required 6,8-diododibenz[*a,j*]anthracenes via a double iodonium-induced electrophilic cyclization.^{17,18} Numerous attempts to convert the diiodide to the *bis*-acetylene **5** via Sonogashira and Castro-Stephens reactions proved unsuccessful, instead resulting in complex, undefined mixtures. However, an indirect method involving a lithiation/carbonylation sequence to give **4**, followed by Corey-Fuchs homologation¹⁹, successfully afforded dialkyne **5**. Owing to the sterically encumbered environment of the reaction centers, dialdehyde **4** was always accompanied by the formation of monoaldehyde byproduct **13**. Separation of the two could however, be easily achieved by column chromatography. Finally, an

oxidative coupling utilizing conditions previously developed²⁰ in our group was performed, furnishing macrocycles **6a** and **6b** in reasonable yields.

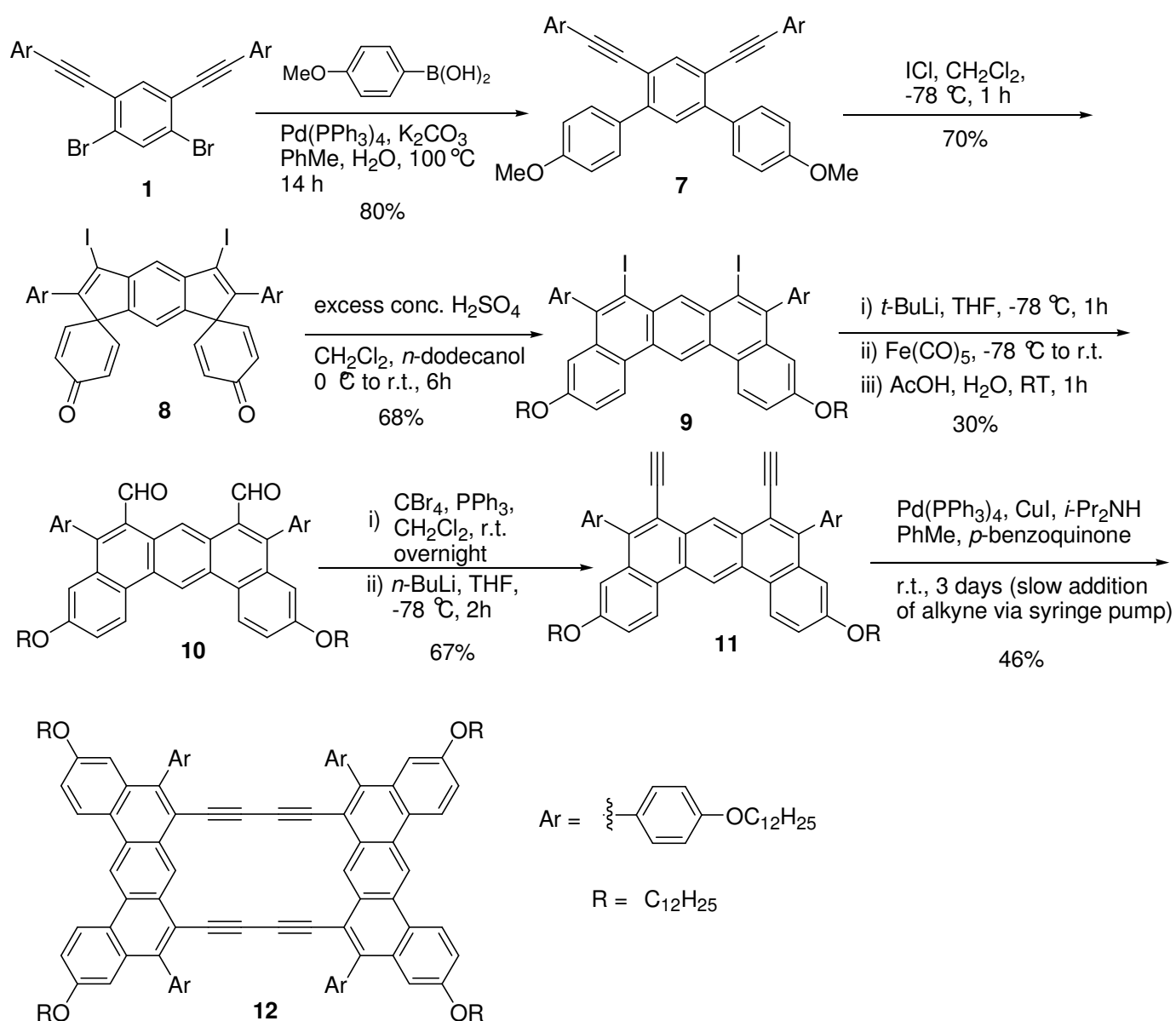
SCHEME 1. Synthesis of macrocycles **6a** and **6b**.



The synthesis of macrocycle **12** (Scheme 2) involved a similar sequence of transformations employed in the preparation of **6a** and **6b**, with the exception that the *bis*-alkoxyterphenyl **7** could only be converted to the desired diiodide **9** in two steps, via a skeletal rearrangement of the structurally intriguing **8**, using modifications of known reactions.^{6, 21} A second alkoxy-based macrocycle bearing branched farnesol-derived sidechains was also synthesized in a manner analogous to **12**, with its

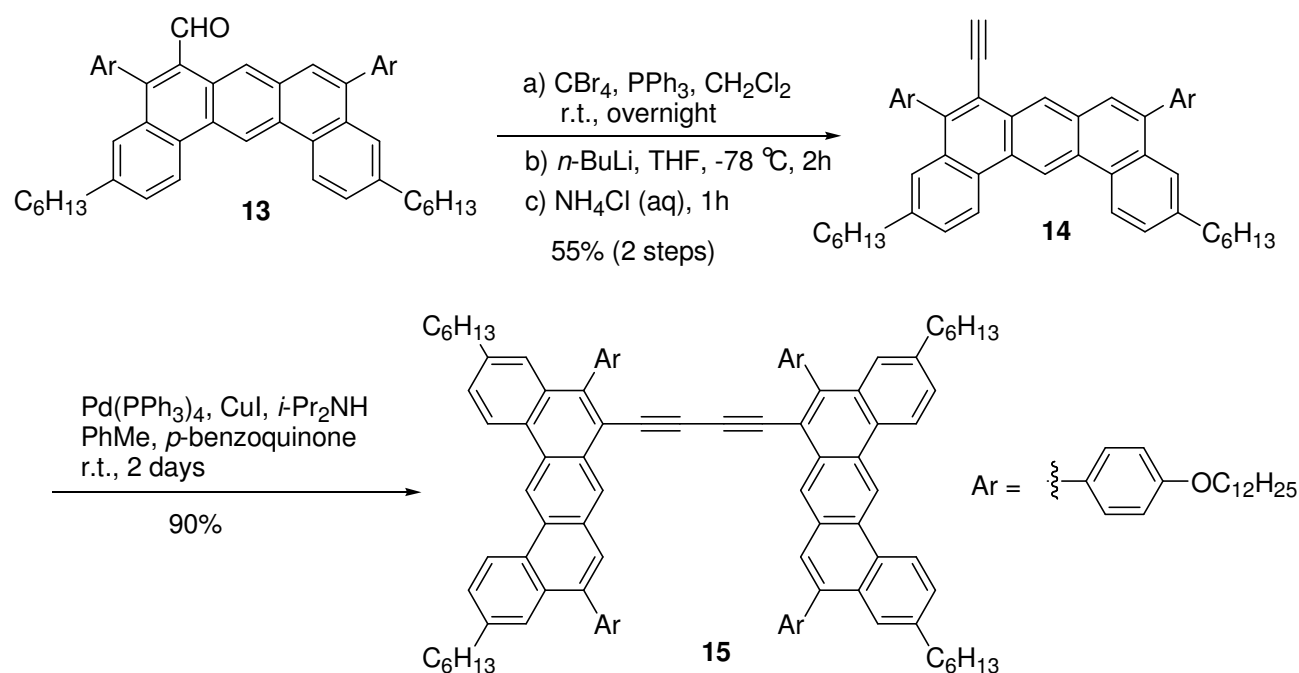
existence confirmed by MALDI-TOF. Unfortunately, this fourth and final macrocycle could not be satisfactorily separated from a trimeric byproduct even after repeated column chromatography and attempted fractional recrystallizations. In addition to the three macrocycles, compound **15** (the acyclic analog of **6a**) was also prepared to study the effect of the number of bridges on the photophysical properties. This was made in three steps (Scheme 3) starting from monoaldehyde **13**, which is a byproduct isolated during the purification of dialdehyde **4a**.

SCHEME 2. Synthesis of macrocycle **12**.



The abovementioned target compounds were characterized by ^1H NMR, ^{13}C NMR, high-resolution mass spectrometry (MALDI-TOF), UV/Vis and fluorescence spectroscopy. In the ^1H NMR spectra of the macrocycles, the two protons located within the ring were found to be shifted downfield ($\delta \approx 9.5$ ppm) as a result of Van der Waals deshielding brought about by steric interactions. The lack of any upfield shift of those internal protons implies the absence of a ring current²² in these systems (i.e. no diatropic effect observed). Brief polarized optical microscopy experiments were also performed on the macrocycles in hope of finding liquid crystalline behavior as well, but the compounds had extremely high melting points (between 200°C and 330°C) and were also observed to decompose and discolor at those elevated temperatures.

SCHEME 3. Synthesis of acyclic **15**.

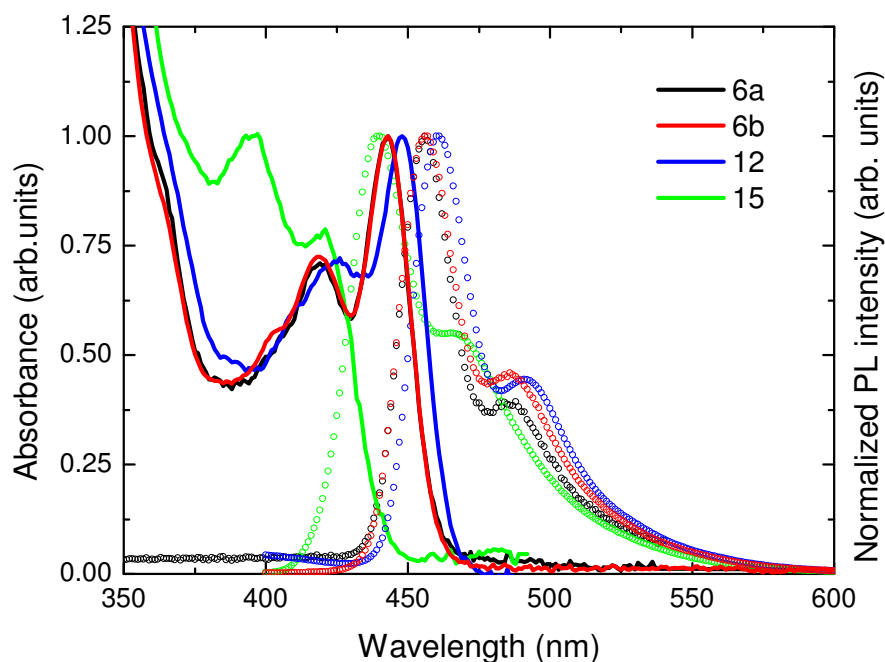


Photophysical studies. A SPEX fluorolog, with dual monochromators, was used to collect photoluminescence (PL) and photoluminescence excitation (PLE) spectra. The instrument is wavelength and intensity calibrated and it compensates for variations in excitation intensity by monitoring the incident optical power level. In PL measurements, the **6a** films were optically excited at a wavelength $\lambda = 375$ nm. For PLE spectra, emission at $\lambda = 508$ nm was collected. Figure 1 shows the UV-Vis absorption and fluorescence spectra of the four compounds in chloroform. Macrocycles **6a** and

6b displayed essentially identical spectral profiles, with absorption and emission maxima occurring at around 440 nm and 455 nm respectively. Changing the peripheral alkyl groups to alkoxy chains (e.g. **12**) resulted in a slight bathochromic shift, with the spectral shape remaining similar otherwise. The spectra of the acyclic **15** differed somewhat from the macrocycles, which was expected due to the major structural difference. Its absorption spectrum was blue-shifted relative to the others, possibly due to reduced conjugation resulting from the absence of the second diyne linker. A much larger Stokes shift was also observed, which could indicate reduced rigidity, once again as a result of having only a single linker. Fluorescence quantum yields of the compounds were measured against quinine sulfate in 0.1N H₂SO₄ (Table 1). The three macrocycles in chloroform solution showed fairly high quantum yields between 0.40 and 0.50, whereas the singly-bridged **15** had a lower value of 0.35.

Table 1. Photophysical properties of **6a**, **6b**, **12**, and **15**.

Compound	Absorption max (nm)	Emission max (nm)	Quantum yield, Φ_F	Extinction coefficient ($M^{-1} cm^{-1}$)
6a	443	456	0.45	90141 (at 443 nm)
6b	443	456	0.43	63569 (at 443 nm)
12	448	461	0.47	79113 (at 448 nm)
15	395	440	0.35	38206 (at 395 nm)



1
2
3
4
5
6
7
8
9
10
11
12
13
14
15
16
17
18
19
20
21
22
23
24
25
26
27
28
29
30
31
32
33
34
35
36
37
38
39
40
41
42
43
44
45
46
47
48
49
50
51
52
53
54
55
56
57
58
59
60

FIGURE 1. Normalized absorbance (solid lines) and emission (dotted lines) spectra of **6a**, **6b**, **12** and **15** in chloroform.

To test for the presence of J-aggregates, we investigated the thin film photophysics of the macrocycles. As **6a** was synthesized in the largest quantity, films of this compound were studied in greatest detail. The initial films were produced by spin-coating a fairly concentrated (5 mg/mL) toluene solution of **6a** on to glass or quartz cover-slips (18 x 18 mm). Fortuitously, the first few films showed promising UV-Vis absorption features consistent with J-aggregates (Figure 2).

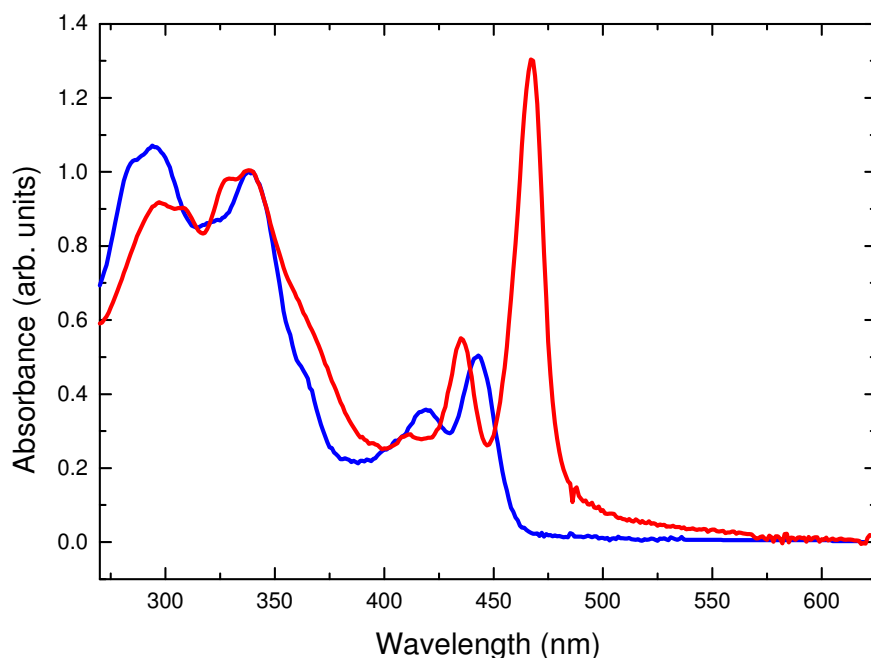


FIGURE 2. Absorption spectra of **6a**, solution (blue line) vs. film (red line), normalized to the absorbance at 340 nm.

Compared with the solution spectrum, the **6a** film spectrum shows an aggregate absorption peak at 467 nm (red-shifted by 23 ± 1 nm from the solution). Even more notable is the high intensity and narrow linewidth of this peak (J-band), which dominates all other spectral features. This is in stark contrast to the solution spectrum, in which the peak at 443 nm shows much lower intensity than those between 300 nm and 360 nm (absorptions due to pendant *p*-alkoxyphenyl moieties). Normalizing the solution and film absorbances at 340 nm, the enhancement in the peak intensity (at 467 nm) relative to the other spectral features becomes evident (Figure 2). The bathochromic shift and the strong intensity

of the aggregate peak, are photophysical characteristics of J-aggregates.²³ From the emission spectra of the **6a** films we find the Stokes shift to be only 4 nm (Figure 3), versus 13 nm in solution phase. Such minimal Stokes shift is also consistent with the existence of J-aggregates.²⁴ It is notable that the fluorescence band is a mirror image of the low energy edge of the J-band absorption.

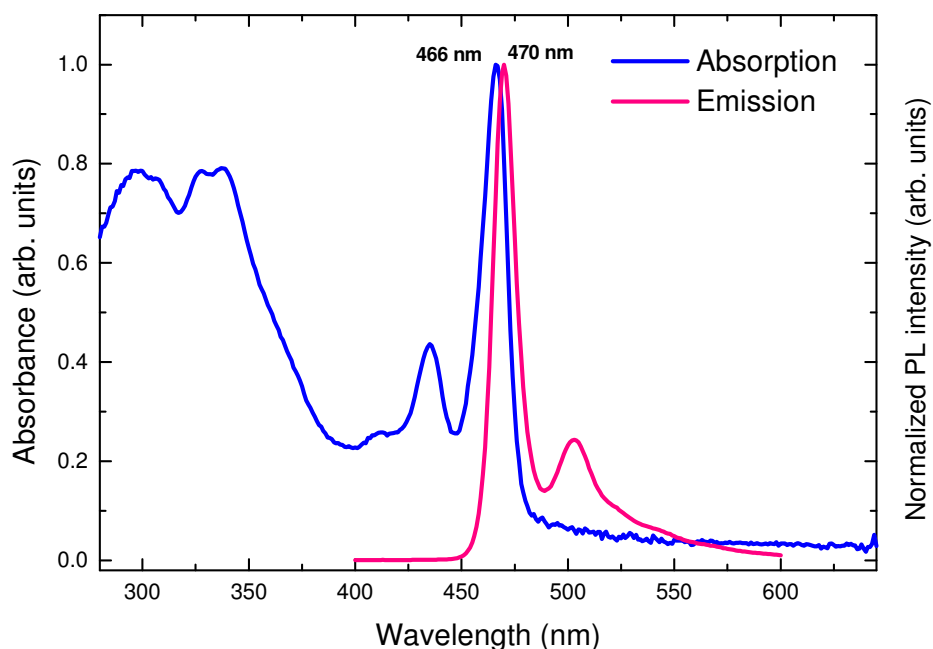


FIGURE 3. Normalized absorption (blue line) and fluorescence (pink line) spectra of **6a** (film).

We also find that it is possible to spin-coat films of **6a** that did not display a J-band. These less strongly absorbing films could be produced when: the spin rate (of the spin-coating process) was high (e.g. 4000 rpm), a lower concentration (< 2 mg/mL) of **6a** in solvent was used, or when a more volatile solvent (e.g. THF) was employed. The use of these parameters provided for less-than-favorable conditions for aggregate formation. But when these ‘non-aggregated’ (i.e. monomeric) films were then subjected to conditions conducive to aggregate formation, the typical J-aggregate spectral features were found to emerge with time. This was achieved by vapor-annealing the films in a solvent chamber saturated with toluene vapor for 45 minutes, and then retrieving them for spectral (UV-Vis) re-acquisition. It can be seen (Figure 4) that the vapor-annealing, which should result in more ordered thin films²⁵, precipitates the appearance of the highly intense J-band, confirming that molecular organization

1
2
3
4
5
6
7
8
9
10
11
12
13
14
15
16
17
18
19
20
21
22
23
24
25
26
27
28
29
30
31
32
33
34
35
36
37
38
39
40
41
42
43
44
45
46
47
48
49
50
51
52
53
54
55
56
57
58
59
60

was indeed important in producing the desired J-aggregate photophysics. When the volatile THF is used as the spin-casting solvent (particularly with low **6a** concentration) the resulting films lacked J-aggregate features. However, J-aggregate features can be recovered when these films are placed in a solvent chamber containing THF vapor (Figure 4).

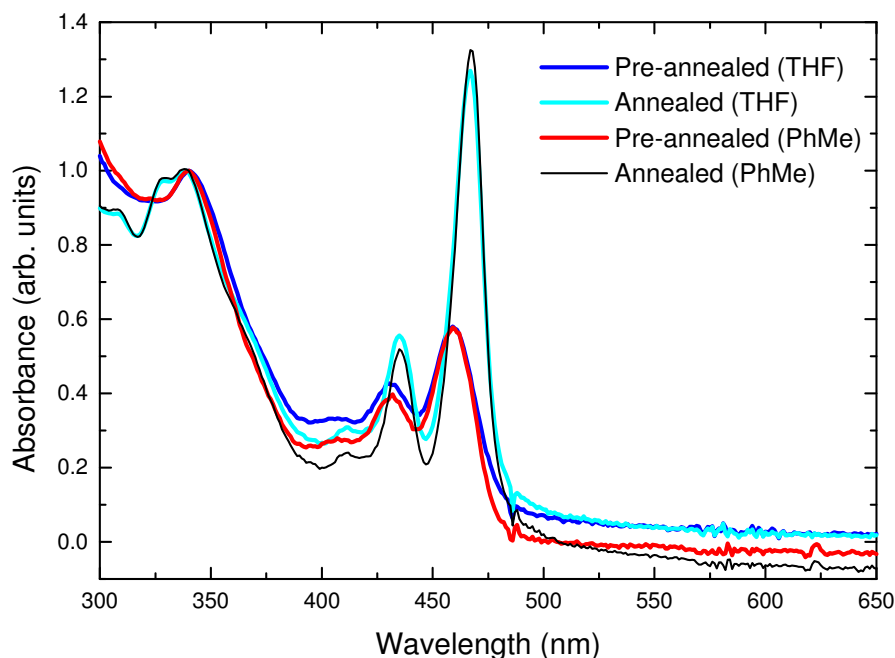


FIGURE 4. Absorption spectra of **6a** (film), before and after annealing under toluene (PhMe) and THF vapor, normalized to the absorbance at 340 nm.

Similar photophysical experiments were also performed on films of the two longer-chained macrocyclic analogs **6b** and **12**. In both cases, the films are cast from THF solutions of the macrocycles, and subsequently annealed under THF vapor for 45 minutes. UV-Vis data are acquired before and after the annealing process, and the spectra of **6b** and **12** are shown in Figure 5. The spectra of the pre-annealed films did not show J-bands, but these appeared in both cases upon annealing. Therefore, the results obtained with **6b** and **12** were analogous to those of **6a**, suggesting that the doubling of chain length of the peripheral alkyl/alkoxy groups had little effect on the photophysics, be it in solution or in the film-state. Similar J-aggregate photophysics could not be observed with the non-cyclic **15**, implying that the aggregate formation may require approximate molecular planarity (steric hindrance in the non-cyclic **15** produces a larger deviation from planarity, since the two dibenzanthracene sub-units are less

constrained). It is likely that J-aggregation of these polycyclic aromatics in the solid-state relies on π - π stacking interactions that could be disrupted if the non-planarity became too pronounced.

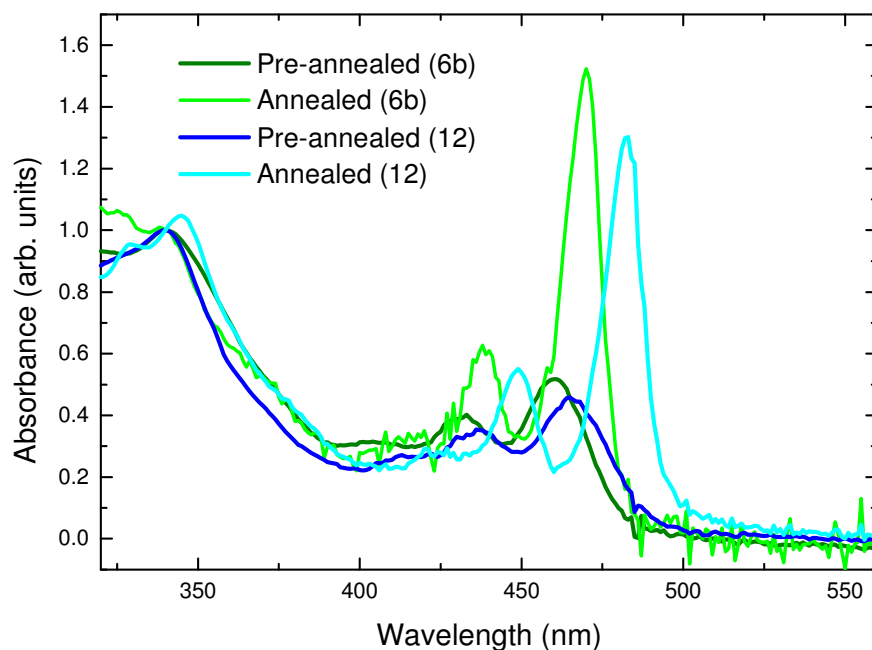


FIGURE 5. Absorption spectra of **6b** (film) and **12** (film), before and after annealing under THF vapor, normalized to the absorbance at 340 nm.

Additional experiments examining the photophysics of **6a** as a function of concentration were also undertaken. A series of films were spin-coated using **6a** solutions (polyisobutylene matrix /chlorobenzene as solvent) of varying concentrations, and their photoluminescence spectra, excitation spectra, and fluorescence lifetimes were measured. Chlorobenzene was chosen as it provided for optimal co-miscibility of **6a**, polyisobutylene, and solvent. When a film containing a very low concentration of **6a** (i.e. 0.0005 mg in a 1 mL solution of 40 mg/mL polyisobutylene (PIB) in chlorobenzene) was used, its emission peak was at 455 nm (Figure 6), identical to that observed in solution spectra. As the amount of **6a** used in the spin-coating process was increased to 0.002 mg/mL of PIB/chlorobenzene, aggregate peaks began to emerge at 470 nm with a shoulder at 500 nm, while the 455 nm “monomer” peak diminished. A further increase in **6a** concentration to 0.005 mg/mL resulted in further reduction in the 455 nm peak, so that at 0.02 mg/mL the monomer peak can no longer be observed, at which point the emission spectrum begins to resemble those obtained with neat films discussed above (pure **6a**, no PIB

1 matrix). From the excitation spectra (Figure 7), no J-band at 470 nm could be observed at the lowest
2 concentration of 0.0005 mg/mL, but as the concentration was increased ten-fold, a peak at 470 nm
3 appeared, becoming more pronounced with increasing **6a** concentrations. Fluorescence lifetimes (at 470
4 nm) for a series of solutions and films of different concentrations were also measured. Solution lifetimes
5 were found to be between (1.7 ± 0.1) ns regardless of concentration. In the film state, it can be observed
6 from Table 2 that the lifetimes generally decrease as the concentration of **6a** was increased from 0.0005
7 to 2.000 mg/mL (only a small incidence of scatter is observed in the trends). In particular, with a
8 concentration of 0.0005 mg/mL, a lifetime of $\tau_m = 1.3$ ns was obtained, comparable to what was
9 observed in chlorobenzene solutions, while at higher concentrations, lifetimes of about $\tau_f = 0.24$ ns are
10 observed. Higher doping concentration also leads to a measureable increase in thin film
11 photoluminescence (PL) quantum yield (QY) from $\Phi_m = 43 \pm 6 \%$ for the monomeric film to $\Phi_f = 92 \pm$
12 8% for the aggregate films. To determine PL QY, we compared the PL counts from the **6a** film to a
13 thin film standard of known QY, accounting for relative differences in absorption strength of the films.
14 The standard was a thin film of thickness 75 nm of the small molecule *tris*(8-
15 hydroxyquinolinato)aluminum (Alq_3). The Alq_3 film was prepared by thermally evaporating re-
16 crystallized Alq_3 in ultra high vacuum (growth pressure below 10^{-6} Torr) onto a quartz substrate that was
17 carefully solvent cleaned and oxygen plasma treated to remove trace impurities. The published QY for
18 Alq_3 in thin film is $32 \pm 2\%$.²⁶ We erred on the side of caution and used a value of QY = 30% for our
19 calculations. To make a fair comparison of QY, for each film in consideration, the percentage of
20 absorbed optical excitation was determined from optical transmission measurements. Measured PL
21 counts were then normalized to the percent absorption values, on a film by film basis. For **6a** in
22 monomeric form, we calculated the PL QY to be $43 \pm 6 \%$, which is similar to the QY for **6a** in solution,
23 and for **6a** at high doping concentrations, we determined the QY to be $92 \pm 8 \%$.

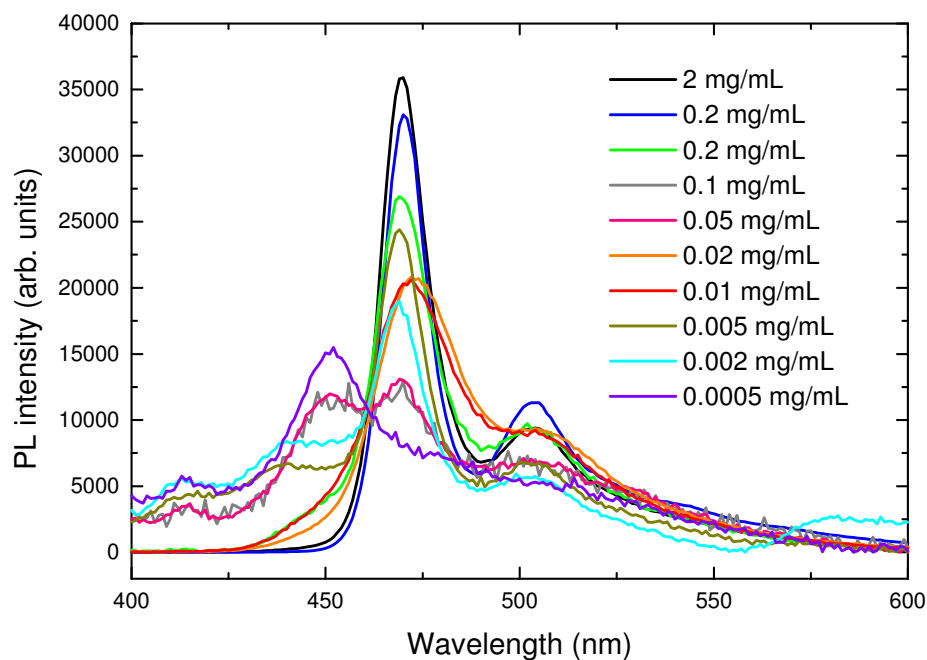
24 The emergence of a red-shifted narrower linewidth optical transition at higher **6a** concentrations,
25 the corresponding reduction in lifetime, and increase in quantum yield of aggregates as compared to
26
27
28
29
30
31
32
33
34
35
36
37
38
39
40
41
42
43
44
45
46
47
48
49
50
51
52
53
54
55
56
57
58
59
60

1 monomers are indicative of J-aggregate formation.²⁷ In J-aggregates, strong coupling between the
2 monomer transition dipoles produces a new cooperative molecular state. The coupling results in a new
3 optical transition called the J-band, when the interaction strength exceeds the monomeric dephasing
4 processes.²⁸ The interaction between monomeric transition dipoles lowers the overall energy of the
5 cooperative state; hence the J-band absorption/fluorescence is red-shifted relative to that of the
6 monomer. In the J-aggregate state, multiple molecules coherently couple, the number being denoted by
7 N_c , and the J-aggregate exciton delocalizes over all of them.²⁹ Coherent coupling amongst the N_c
8 molecules leads to the acceleration of the radiative rate of the J-band states by a factor of N_c relative to
9 the monomer,³⁰ which translates into shorter excited state lifetime and higher PL QY. The radiative rate
10 enhancement is typically referred to as a superradiance phenomenon since it is caused by coherent
11 exciton coupling,³¹ though in J-aggregates the mechanism for the coupling is near-field Coulombic
12 interactions while in classic superradiant systems, the origin is interference effects in the spontaneous
13 light emission process.³² Since the radiative rate of a J-aggregate increases relative to that of the
14 monomer by a factor of N_c , from a comparison of lifetimes (τ_J vs. τ_m) and quantum yields (Φ_J vs. Φ_m),
15 N_c can be determined using the equation³³:

$$N_c = \frac{\tau_m \Phi_J}{\tau_J \Phi_m}$$

16 The data obtained suggest that N_c is on the order of 12 for our **6a** J-aggregate films. Coherent coupling
17 also leads to a narrower total linewidth for the J-aggregate optical transition relative to the monomer,
18 because the delocalized exciton averages out site-to-site variations, and suppresses the inhomogeneous
19 broadening.³⁴ The linewidths of the monomer optical transition and the J-band are dominated by
20 inhomogeneous broadening. Nevertheless, the width of the J-band relative to the monomer spectrum
21 does characterize the coherence of the system. The linewidth of the J-band is narrower than the
22 monomer optical transition because in the J-aggregate state, the exciton is delocalized over the N_c
23 molecules that are coherently coupled, which tends to average out site-to-site inhomogeneities in the
24 exciton energy. This motional narrowing is manifest in the smaller linewidth for J-aggregate absorption
25
26
27
28
29
30
31
32
33
34
35
36
37
38
39
40
41
42
43
44
45
46
47
48
49
50
51
52
53
54
55
56
57
58
59
60

1 and emission spectra. This coherent coupling also results in the accelerated radiative process in the J-
2 aggregate state, which translates into the higher observed QY and shorter exciton lifetime for the J-
3 aggregate compared to the monomer.
4
5 aggregate compared to the monomer.
6
7
8
9



33 **FIGURE 6.** Photoluminescence intensity vs. concentration of **6a** in thin films (PL scaled by subtracting
34 the background and scaling by integrated intensity at all wavelengths).
35
36
37
38
39
40
41
42
43
44
45
46
47
48
49
50
51
52
53
54
55
56
57
58
59
60

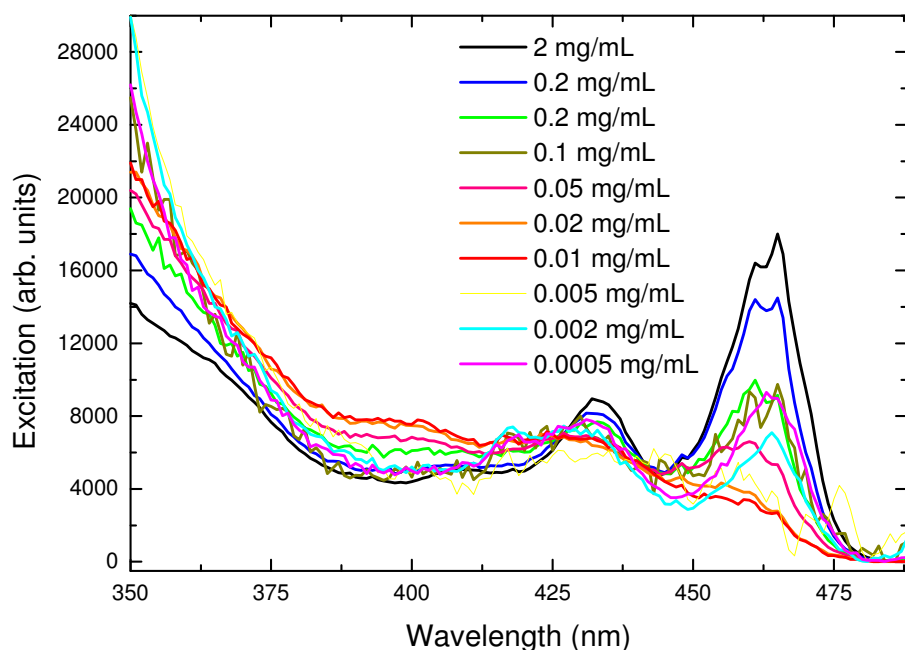


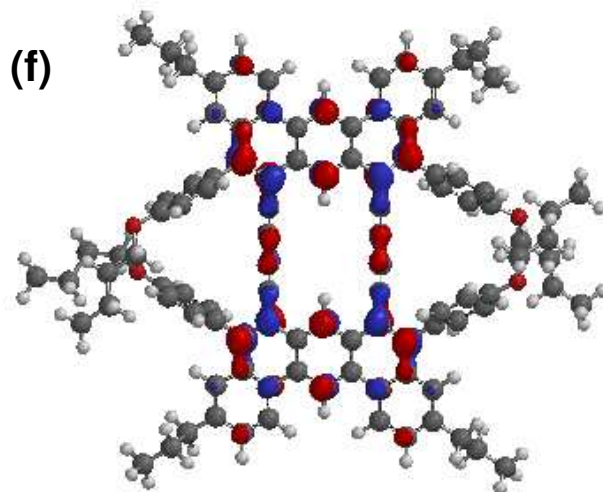
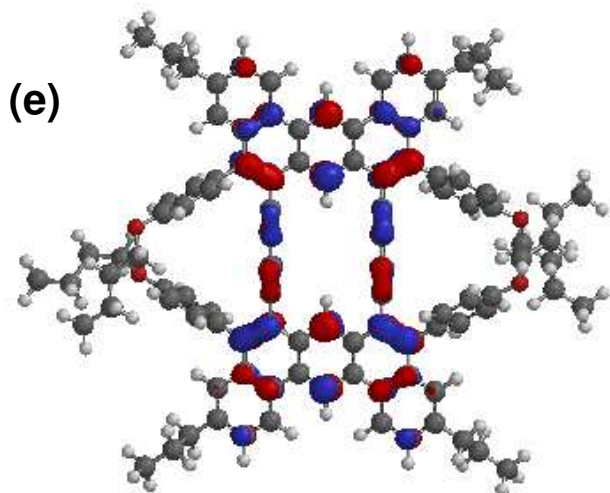
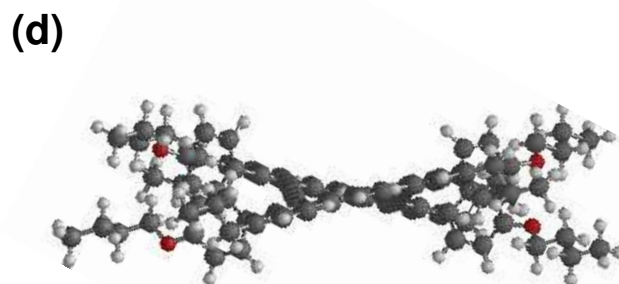
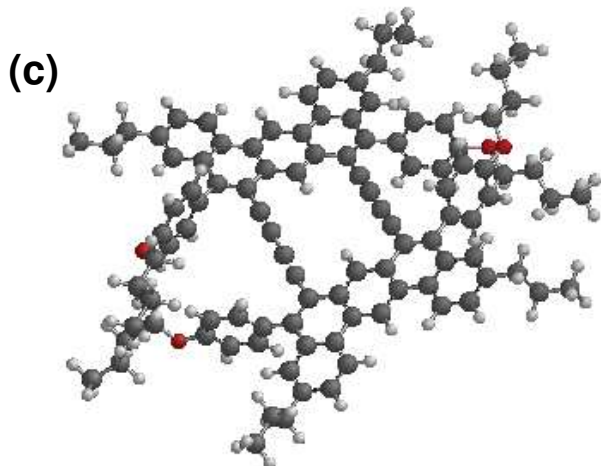
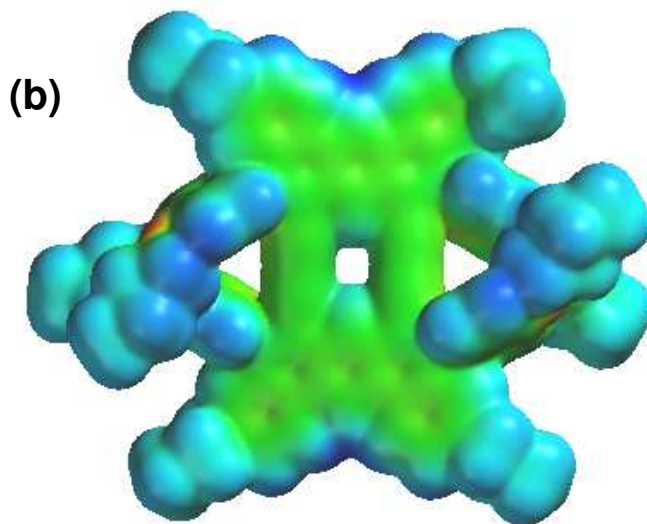
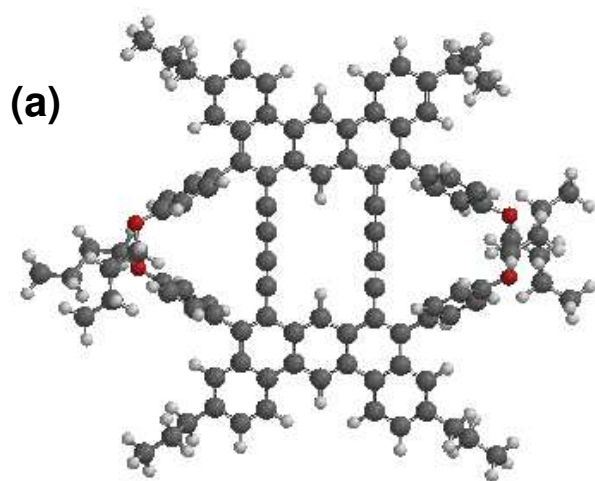
FIGURE 7. Excitation vs. concentration of **6a** in thin films (PLE scaled by subtracting background and scaling by integrated intensity at all wavelengths).

Table 2. Fluorescence lifetimes of **6a** (solutions and films) at different concentrations.

Concentration (mg/mL)	Lifetimes (bimodal) (ns)		State
0.002	1.7 (100%)	-	Solution (PhCl)
0.02	1.7 (100%)	-	Solution (PhCl)
0.2	1.8 (100%)	-	Solution (PhCl)
0.0005	1.3 (99.9%)	4.8 (0.1%)	Film
0.002	0.2 (96.7%)	1.3 (3.3%)	Film
0.005	0.3 (96.6%)	1.2 (3.4%)	Film
0.01	0.3 (97.4%)	1.0 (2.6%)	Film
0.02	0.2 (98.1%)	1.1 (1.9%)	Film
0.05	0.6 (84.5%)	1.5 (15.5%)	Film
0.10	0.4 (82.7%)	1.4 (17.3%)	Film
0.20	0.4 (94.9%)	1.4 (5.1%)	Film
2.00	0.2 (97.4%)	0.7 (2.6%)	Film

Molecular modelling. In order to better visualize the equilibrium geometry of the macrocycles **6a**, **6b**, and **12**, molecular calculations³⁵ were performed at the semi-empirical PM3 level, using a model

1 compound (Figure 8) with deliberately shortened alkyl sidechains to enable more rapid completion of
2 the calculation. As can be seen in Figure 8, the macrocycle is composed of two 1,3-butadiyne-linked
3 planar dibenz[*a,j*]anthracene sub-units that are slightly staggered relative to each other as a result of
4 steric crowding in the middle of the molecule. Despite this structural distortion, the core of the
5 macrocycle retains some overall planarity, which would still allow for intermolecular π - π stacking
6 interactions. By comparison, the acyclic analog shows greater non-planarity (Figure 8g), since the two
7 non-restrained aromatic sub-units have more freedom to minimize steric repulsions. As a result, π - π
8 stacking interactions in acyclic **15** may be weakened.
9
10
11
12
13
14
15
16
17
18
19
20
21
22
23
24
25
26
27
28
29
30
31
32
33
34
35
36
37
38
39
40
41
42
43
44
45
46
47
48
49
50
51
52
53
54
55
56
57
58
59
60



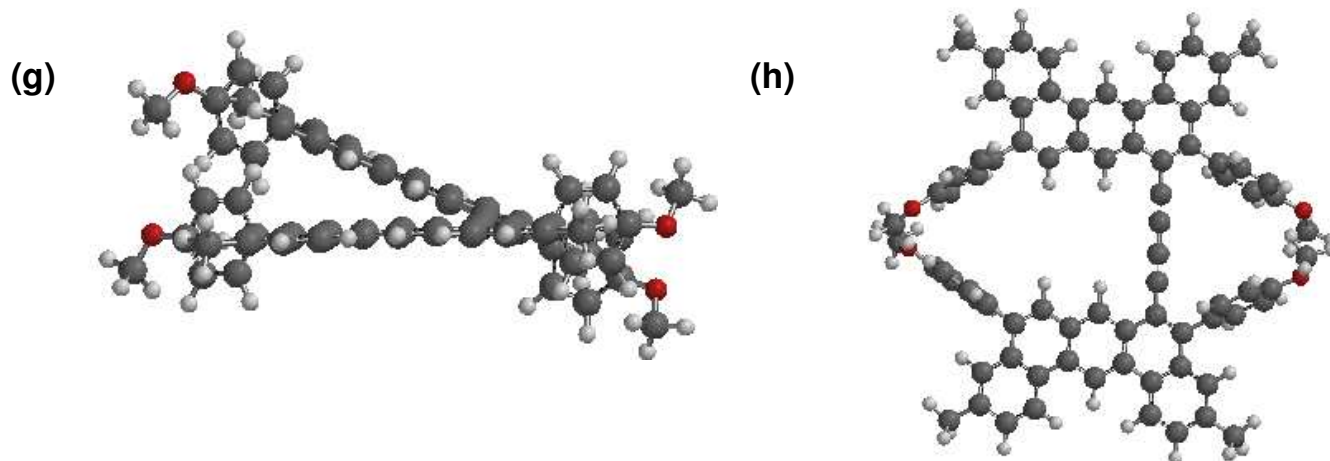


FIGURE 8. PM3-calculated models (a) top-down view of geometry-optimized macrocyclic structure, (b) molecular electrostatic potential map, (c) optimized structure tilted to emphasize steric crowding, (d) edge-on view of optimized structure, (e) frontier HOMO, and (f) frontier LUMO, (g) edge-on view of the acyclic model structure, (h) top-down view of the acyclic structure.

CONCLUSION. In summary, three dibenz[*a,j*]anthracene-based macrocycles have been synthesized and spectroscopically characterized. The conjugated macrocycles display pronounced photophysical properties in the solid-state, such as the intense red-shifted absorbances, narrow linewidths, and small Stokes shifts, indicating J-aggregate formation. These new compounds may have the potential to be utilized in various optoelectronic devices (e.g. lasers, photovoltaics, and polaritonic devices^{16a, 36}).

ACKNOWLEDGMENT. This work was supported by the National Science Foundation and the Army Research Office's IED Stand-Off Detection Research Program (W911NF-07-1-0654), and the U.S. Army through the Institute for Soldier Nanotechnologies (DAAD-19-02-0002).

SUPPORTING INFORMATION AVAILABLE: Full experimental details pertaining to the synthesis of all new compounds described herein. This information is available free of charge via the Internet at <http://pubs.acs.org>.

REFERENCES

- [1] a) Sakamoto, J.; Schlüter, A. D.; *Eur. J. Org. Chem.* **2007**, 2700-2712; b) Zhang, W.; Moore, J. S. *Angew. Chem. Int. Ed.* **2006**, 45, 4416-4439; c) Kumar, S. *Chem. Soc. Rev.* **2006**, 35, 83-109.
- [2] Akiyama, S.; Misumi, S.; Nakagawa, M. *Bull. Chem. Soc. Jpn.* **1960**, 33, 1293-1298.

- [3] a) Toyota, S.; Goichi, M.; Kotani, M. *Angew. Chem. Int. Ed.* **2004**, *43*, 2248-2251; b) Toyota, S.; Kurokawa, M.; Araki, M.; Nakamura, K.; Iwanaga, T. *Org. Lett.* **2007**, *9*, 3655-3658; c) Goichi, M.; Toyota, S. *Chem. Lett.* **2006**, *35*, 684-685; d) Goichi, M.; Segawa, K.; Suzuki, S.; Toyota, S. *Synthesis* **2005**, *13*, 2116-2118; e) Toyota, S.; Goichi, M.; Kotani, M.; Takezaki, M. *Bull. Chem. Soc. Jpn.* **2005**, *78*, 2214-2227; f) Toyota, S.; Suzuki, S.; Goichi, M. *Chem. Eur. J.* **2006**, *12*, 2482-2487.
- [4] a) Taylor, M. S.; Swager, T. M. *Angew. Chem. Int. Ed.* **2007**, *46*, 8480-8483; b) Bunz, U. H. F. *Chem. Rev.* **2000**, *100*, 1605-1644; c) Becker, K.; Lagoudakis, P. G.; Gaefke, G.; Höger, S.; Lupton, J. M. *Angew. Chem. Int. Ed.* **2007**, *46*, 1; d) Marsden, J. A.; Haley, M. M. *J. Org. Chem.* **2005**, *70*, 10213-10226.
- [5] a) Grimsdale, A. C.; Wu, J.; Müllen, K. *Chem. Commun.* **2005**, 2197-2204; b) Tyutyulkov, N.; Müllen, K.; Baumgarten, M.; Ivanova, A.; Tadjer, A. *Synth. Met.* **2003**, *139*, 99-107; c) Simpson, C. D.; Brand, J. D.; Berresheim, A. J.; Przybilla, L.; Rader, H. J.; Müllen, K. *Chem. Eur. J.* **2002**, *8*, 1424-1429; d) Ito, S.; Wehmeier, M.; Brand, J. D.; Kubel, C.; Epsch, R.; Rabe, J. P.; Müllen, K. *Chem. Eur. J.* **2000**, *6*, 4327-4342.
- [6] a) Zhang, X.; Larock, R. C. *J. Am. Chem. Soc.* **2005**, *127*, 12230-12231; b) Yao, T.; Campo, M. A.; Larock, R. C. *J. Org. Chem.* **2005**, *70*, 3511-3517.
- [7] a) Würthner, F. *Chem. Commun.* **2004**, 1564-1579; b) Würthner, F. *Pure Appl. Chem.* **2006**, *78*, 2341-2349.
- [8] a) Holzwarth, A. R., Schaffner, K. *Photosynth. Res.* **1994**, *41*, 225-233; b) McDermott, G., Prince, S. M., Freer, A. A., Hawthornthwaite-Lawless, A. M., Papiz, M. Z., Cogdell, R. J., Isaacs, N. W. *Nature* **1995**, *374*, 517-521; c) Pullerits, T., Sundström, V. *Acc. Chem. Res.* **1996**, *29*, 381-389; d) Balaban, T. S., Tamiaki, H., Holzwarth, A. R. *Top. Curr. Chem.* **2005**, *258*, 1-38.
- [9] a) Takahashi, R., Kobuke, Y. *J. Am. Chem. Soc.* **2003**, *125*, 2372-2373; b) Yamaguchi, T., Kimura, T., Matsuda, H., Aida, T. *Angew. Chem. Int. Ed.* **2004**, *43*, 6350-6355; c) Elemans, J. A. A. W., van Hameren, R., Nolte, R. J. M., Rowan, A. E. *Adv. Mater.* **2006**, *18*, 1251-1266; d) Wang, H., Kaiser, T. E., Uemura, S., Würthner, F. *Chem. Commun.* **2008**, 1181-1183.
- [10] a) Kaiser, T. E., Wang, H., Stepanenko, V., Würthner, F. *Angew. Chem. Int. Ed.* **2007**, *46*, 5541-5544; b) Yagai, S., Seki, T., Karatsu, T., Kitamura, A., Würthner, F. *Angew. Chem. Int. Ed.* **2008**, *47*, 3367-3371; c) Li, X.-Q., Zhang, X., Ghosh, S., Würthner, F. *Chem. Eur. J.* **2008**, *14*, 8074-8078; d) Würthner, F., Bauer, C., Stepanenko, V., Yagai, S. *Adv. Mater.* **2008**, *20*, 1695-1698.
- [11] a) Kobayashi, T., Ed. *J-Aggregates*; World Scientific: Singapore 1996. b) Möbius, D. *Adv. Mater.* **1995**, *7*, 437-444.
- [12] Borsenberger, P. M., Chowdry, A., Hoesterey, D. C., Mey, W. *J. Appl. Phys.* **1978**, *44*, 5555-5564.
- [13] Chatterjee, S., Davis, P. D., Gottschalk, P., Kurz, M. E., Sauerwein, B., Yang, X., Schuster, G. B. *J. Am. Chem. Soc.* **1990**, *112*, 6329-6338.
- [14] a) Wang, Y. *Chem. Phys. Lett.* **1986**, *126*, 209-214; b) Wang, Y. *J. Opt. Soc. Am. B.* **1991**, *8*, 981-985; c) Kobayashi, S. *Mol. Cryst. Liq. Cryst.* **1992**, *217*, 77-81.

- 1
2
3
4
5
6
7
8
9
10
11
12
13
14
15
16
17
18
19
20
21
22
23
24
25
26
27
28
29
30
31
32
33
34
35
36
37
38
39
40
41
42
43
44
45
46
47
48
49
50
51
52
53
54
55
56
57
58
59
60
- [15] Tischler, J. R., Bradley, M. S., Bulović, V. *Opt. Lett.* **2006**, *31*, 2045-2047.
- [16] a) Tischler, J. R., Bradley, M. S., Bulović, V., Song, J. H., Nurmikko, A. *Phys. Rev. Lett.* **2005**, *95*, 036401; b) Tischler, J. R., Bradley, M. S., Zhang, Q., Atay, T., Nurmikko, A., Bulović, V. *Org. Electron.* **2007**, *8*, 94-113.
- [17] Goldfinger, M. B.; Crawford, K. B.; Swager, T. M. *J. Am. Chem. Soc.* **1997**, *119*, 4578-4593.
- [18] Goldfinger, M. B.; Khushrav, K. B.; Swager, T. M. *J. Org. Chem.* **1998**, *63*, 1676-1686.
- [19] a) Corey, E. J.; Fuchs, P. L. *Tetrahedron Lett.* **1972**, 3769-3772; b) Ramirez, F.; Desai, N. B.; McKelvie, N. *J. Am. Chem. Soc.* **1962**, *84*, 1745-1747.
- [20] Williams, V. E.; Swager, T. M. *J. Polym. Sci., Part A: Polym. Chem.* **2000**, *38*, 4669-4676.
- [21] Li, C.-W.; Wang, C.-I.; Liao, H.-Y.; Chaudhuri, R.; Liu, R.-S. *J. Org. Chem.* **2007**, *72*, 9203-9207.
- [22] a) Fowler, P. W.; Lillington, M.; Olson, L. P. *Pure Appl. Chem.* **2007**, *79*, 969-980; b) Boydston, A. J.; Haley, M. M.; Williams, R. V.; Armantrout, J. R. *J. Org. Chem.* **2002**, *67*, 8812-8819; c) Soncini, A.; Domene, C.; Engelberts, J. J.; Fowler, P. W.; Rassat, A.; van Lenthe, J. H.; Havenith, R. W. A.; Jenneskens, L. W. *Chem. Eur. J.* **2005**, *11*, 1257-1266; d) Lepetit, C.; Godard, C.; Chauvin, R. *New J. Chem.* **2001**, *25*, 572-580.
- [23] a) Jelley, E. E. *Nature* **1936**, *138*, 1009. b) Scheibe, G. *Angew. Chem.* **1936**, *49*, 563.
- [24] Scheibe, G. *Optische Anregung organischer Systeme*, 2. Internationales Farbensymposium, Ed. Foerst, W., Verlag Chemie, Weinheim: 1966, p. 109.
- [25] Mascaro, D. J., Thompson, M. E., Smith, H. I., Bulović, V. *Org. Electron.* **2005**, *6*, 211-220.
- [26] Garbuzov, D. Z.; Bulović, V.; Burrows, P.E.; Forrest, S. R. *Chem. Phys. Lett.* **1996**, *249*, 433-437.
- [27] a) Kuhn, H. *J. Chem. Phys.* **1970**, *53*, 101-108; b) Kirstein, S.; Mohwald, H. *Adv. Mater.* **1995**, *7*, 460-463; c) Peyratout, C.; Daehne, L. *Phys. Chem. Chem. Phys.* **2002**, *4*, 3032-3039.
- [28] Spano, F. C.; Mukamel, S. *J. Chem. Phys.* **1989**, *91*, 683-700.
- [29] Potma, E.O.; Wiersma, D.A. *J. Chem. Phys.* **1998**, *108*, 4894-4903.
- [30] Vanburgel, M.; Wiersma, D.A.; Duppen, K. *J. Chem. Phys.* **1995**, *102*, 20-33.
- [31] a) Spano, F. C.; Kuklinski, J. R.; Mukamel, S. *Phys. Rev. Lett.* **1990**, *65*, 211-214; b) De Boer, S.; Wiersma, D. A. *Chem. Phys. Lett.* **1990**, *165*, 45-53. c) Spano, F. C.; Kuklinski, J. R.; Mukamel, S. *J. Chem. Phys.* **1991**, *94*, 7534-7544. d) Meinardi, F.; Cerminara, M., Sassella, A.; Bonifacio, R.; Tubino, R. *Phys. Rev. Lett.* **2003**, *91*, 247401.
- [32] Dicke, R. H. *Phys. Rev.* **1954**, *93*, 99-110.
- [33] Rousseau, E.; Van der Auweraer, M.; De Schryver, F. C. *Langmuir* **2000**, *16*, 8865-8870.
- [34] Knapp, E. W.; Scherer, P. O. J.; Fischer, S. F. *Chem. Phys. Lett.* **1984**, *111*, 481-486.

1 [35] *Spartan `04 V1.0.0*; Wavefunction, Inc.: Irvine, CA; 2004.

2
3 [36] a) Kena-Cohen, S.; Davanco, M.; Forrest, S. R. *Phys. Rev. Lett.* **2008**, *101*, 116401; b) Holmes, R.
4 J.; Forrest, S. R. *Phys. Rev. Lett.* **2004**, *93*, 186404; c) Lidzey, D. G.; Bradley, D. D. C.; Skolnick,
5 M. S.; Virgili, T.; Walker, S.; Whittaker, D. M. *Nature*, **1998**, *395*, 53-55.
6
7
8
9
10
11
12
13
14
15
16
17
18
19
20
21
22
23
24
25
26
27
28
29
30
31
32
33
34
35
36
37
38
39
40
41
42
43
44
45
46
47
48
49
50
51
52
53
54
55
56
57
58
59
60

Table of Contents Graphic

